# HIGH FREQUENCY METROLOGY FOR INTRACARDIAC ABLATION: IN-VIVO RESULTS

## Amar Rouane[1], Paul Bru[2]

*1) Université de Lorraine, LIEN, EA3440, Nancy, 54000, France (✉ amar.rouane@lien.uhp-nancy.fr, +33383684157);*
*2) Saint Louis Hospital, Cardiology Department, 17019 La Rochelle; France (paul.bru@ch-larochelle.fr; +33546456641)*

**Abstract**

Cardiac Radiofrequency (RF) ablation is a commonly used clinical procedure for treating many cardiac arrhythmias. However, the efficacy of RF ablation may be limited by two factors: small ventricular lesions and impedance rise, leading to coagulum formation and desiccation of tissue. In this paper, a high frequency (HF) energy ablation system operating at 27.12 MHz based on an automated load matching system was developed. A HF energy matched probe associated to the automated impedance matching device ensures optimal transfer of the energy to the load. The aim of this study was to evaluate this energy for catheter ablation of the atrioventricular junction.

*In vivo* studies were performed using 10 sheep to characterize the lesions created with the impedance matching system. No cardiac perforation was noted. No thrombus was observed at the catheter tip. Acute lesions ranged from 3 to 45 mm in diameter (mean ±SD = 10.3±10) and from 1 to 15 mm in depth (6.7±3.9), exhibiting a close relationship between HF delivered power level and lesion size. Catheter ablation using HF current is feasible and appears effective in producing a stable AV block when applied at the AV junction and large myocardial lesions at ventricular sites.

Keywords: impedance matching, voltage measurement cell, current measurement cell, high frequency energy.

## 1. Introduction

RF ablation is used to treat many cardiac arrhythmias [1-3]. However, this technique is more commonly used for treating supraventricular tachycardia [4, 5]. The efficacy of RF ablation however, is limited due to tissue charring and blood coagulation at the electrode [6, 7]. The sudden impedance rise [8, 9] associated with tissue charring and blood coagulation [10] limits prolonged energy delivery, resulting in relatively shallow and small lesions. Therefore, only small lesions are obtained, thus limiting use in ventricular ablation. Several investigators have reported complications and risk during the use of radiofrequency catheter ablation [11-15]. Several researchers have tried to improve the dimensions of these lesions. Certain researchers have worked to improve the protocol [16], or imagine methods of temperature control [17] to prevent reaching tissue temperatures of 90°C. Other teams have developed sources of energy like cryogenics [18], ultrasound [19], laser [20] and microwaves [21-23]. The need for deeper, wider ventricular lesions has led us to develop a high frequency (HF) ablation technique [24]. The therapy efficiency with the electromagnetic signal is determined by optimum energy transfer to the load. On a variable load that is both resistive and capacitive (human body), the relationship between the frequency of applied current and the load is complex.

## 2. Material and method

### 2.1. Material

To follow the evolution of the load, a matching system, Fig. 1, is incorporated between the amplifier and the load in order to optimize the transfer of energy between the generator and the load.
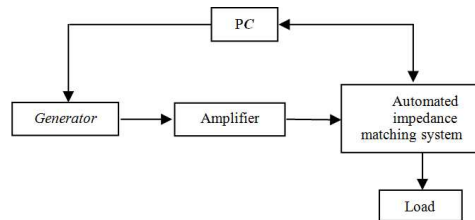
Fig. 1. General schematic of the ablation system.

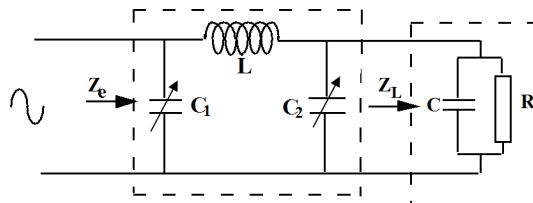The system schematic and the load model are shown in Fig. 2.

Fig. 2. Schematic of the load model.

The load $Z_L$ is modeled by means of a resistance in parallel with a capacitor, Fig. 2. The values of the components ($C_1$ and $C_2$) of the matching system are determined as a function of the average variability of the load. This system was developed to deliver a HF current with automatic impedance matching, Fig. 3, to prevent the power reflection to the generator.
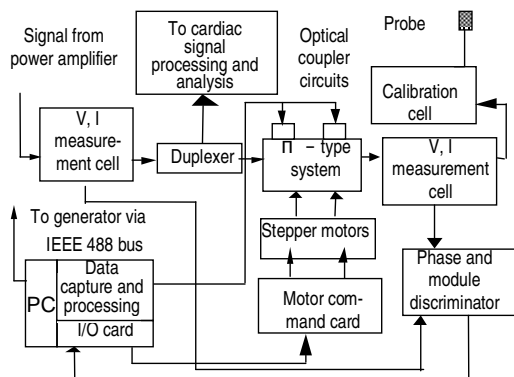
Fig. 3. General schematic of the automation system.

Experimental data concerning energy applied through a specially designed catheter at the AV junction and at ventricular sites is shown. The purpose of this study is to validate the efficacy of the catheter ablation system.

The impedance matching ablation system is a $\pi$ LC network. The coil is fixed [stator], Fig. 2, while the two air-gap capacitors are variable and controlled by stepper motors. The HF current is produced by a low power 0.5-2 W generator that emits a sinusoidal waveform signal at 27.12 MHz. We used a unipolar 7F probe with a 5 mm electrode delivering 100 Watts of power with little energy loss [24-26]. The HF current is delivered by a 5 mm electrode to a large plate on the subject's back. Each application consisted of multiple wave trains delivered at 5 second intervals in order to verify impedance matching [24] until a complete atrioventricular block was achieved. The automated impedance matching system, Fig. 3, is designed around a frequency discriminator/phase detector/modulator supplying the voltage (V) and current (I) modules as well as the phase shift between I and V. The normalized ratio $|V|/|I|$ is determined by an arithmetic operation starting from the data of the modules of V and I. The phase shift is the third impedance matching criterion. When the load is capacitive, the phase shift is <0. When the load is inductive, the phase shift is > 0. When the load is matched, the ratio equals 1 and the phase shift null (standardized impedance).

The HF signal passes through the first current and voltage measurement cells. These two measurement cells are incorporated in the assembly, Fig. 3. The first set, placed before the matching system, checks impedance matching. The second, placed just after the matching system, measures the current through and the voltage across the load, thus making it possible to measure the load impedance. The measuring cells must have minimal insertion losses. Signal loss, in this case, does not exceed 2% to 3%.

*Voltage measuring cell*: Part of the voltage at the HF-input is sampled using a capacitive bridge consisting of the capacitors $C_1$ and $C_2$, Fig. 4. Capacitor $C_2$ is of the adjustable type. $C_1$ is a low-capacitance type that will handle voltages of approximately 500V.
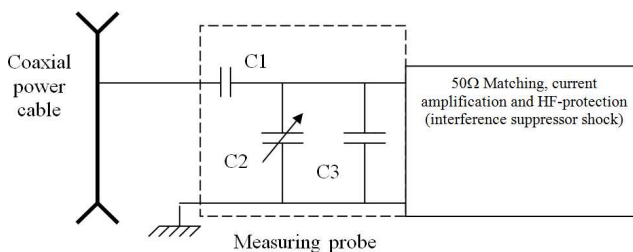


Fig. 4. Voltage probe diagram.

The bridge uses two copper capsules separated by an insulating bakelite printed circuit layer. Measured capacitance $C_1$ at 27.12 MHz is 1 pF.

*Current measuring cell*: The current measuring probe is a ferrite core onto which a transformer is coiled that picks up the HF-induced current, Fig. 5. A divider bridge consisting of $C_1$ and $C_2$ controls the voltage attacking the amplifier.
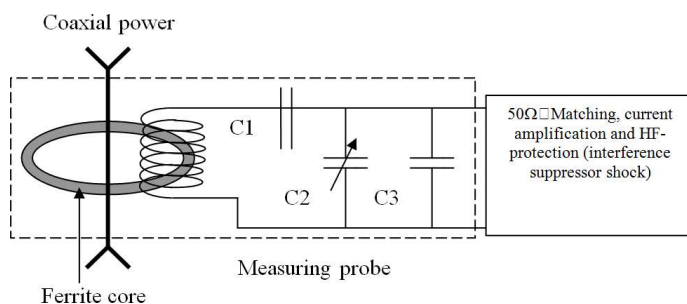


Fig. 5. Current probe diagram.

The current and voltage data sets are sent to the phase and module discriminator which determines the current and voltage modules as well as the relevant phase. These three data are sent to the computer via the I/O card to optimize power transfer. These parameters are:

- The rotation direction of each of the two step motors (not necessarily rotating in the same direction).
- The rotation angles which determine the value of each capacitor.
- The impedance is software-controlled.

Power is entered at the keyboard upon which the direction of rotation of each motor, which determines the capacities, is assessed. The commands are sent from the computer to the stepper motor control card. Before proceeding to the matching process, the air-gap variable capacitors of the π type system are initialized by means of two optical sensors placed on the matching system. The duplexer causes the HF signal to be directed towards the load and the cardiac signal collected by the electrode, a low frequency (LF) signal, to be directed towards the reception and analysis system. Encouraging results were obtained with *in-vitro* experiments [23, 24]. Indeed, these results showed good correlation between the dimensions obtained and the power applied. As they also showed lesion homogeneity, we proceeded to carry out animal experiments in order to validate the HF ablation concept.

## 2.2. Method

Ten adult sheep weighing between 31 and 42 kg were used. The protocol conforms to French and institutional regulatory requirements for invasive studies performed on animals. An intravenous injection of sodium pentobarbital (10 to 30 mg/kg of the animal's weight) was given prior to intubation. General anesthesia was maintained by means of 1.0 and up to 1.5% of halothane, ketamine chlorhydrate under assisted ventilation. Blood was drawn on the same day both before and at the end of the procedure in order to measure creatine kinase (CK-MB), lacticodeshydrogenase, blood count, and to determine standard biochemical blood levels. A standard ECG was monitored throughout the study.

Femoral vein and artery were exposed, allowing insertion of the catheter. First, it was inserted under fluoroscopic guidance into right atrium and ventricle. The catheters are described in detail elsewhere [25]. Unipolar electrocardiograms were band filtered to measure the ST segment elevation. Tracings were displayed on a VR-16 E-M (Electronics for Medicine) oscilloscope and recorded on an Astro-med strip chart recorder. In seven sheep, the catheter was slowly withdrawn from the right ventricle towards the right atrium in order to record the largest His deflection. HF energy was delivered by progressively increasing the power from 10 to 100 Watts (five wave trains of 5 seconds for each energy level) until a complete atrioventricular block was achieved. The energy was then delivered to the right ventricle apex. Immediately after right heart ablation, the catheter was inserted into the femoral artery and directed towards the left ventricle using a retrograde aortic approach. HF energy was delivered at the left ventricular apex. The energy was delivered using 5 wave trains of 5 seconds each; the power level was 60 - 90 Watts in the right and left ventricle, respectively, in the first three animals, then was decreased to between 20-30 Watts for the remaining sheep, as the resulting lesions were too large. In the case of one sheep it was not possible to penetrate the aortic valve and the procedure was stopped. Four sheep were killed at the end of the procedure, to observe the acute pathologic changes. The other six remaining animals were subject to follow-up for 3 weeks. Their ECG was recorded on a weekly basis to evaluate AV conduction. Some animals died during the monitoring period over three weeks. After three weeks, the sheep were euthanized by intravenous injections of chloride of potassium. After death, the entire heart was fixed with 10% formaline and the lesions were stained with Masson's trichrome. Histopathology examination was performed in all cases and

included a macroscopic quantification of the size of the lesions by means of their diameter and maximum depth measurements, and microscopic sections. The sheep were euthanized by intravenous injections of chloride of potassium.

## 3. Results

### 3.1. Atrioventricular junction

The characteristics, parameters and results of the HF application are summarized in Table 1. Ablation of the AV junction was attempted in 7 sheep.

Table 1: Biophysical parameters and results of HF ablation of the AV junction in sheep, VF = Ventricular Fibrillation (heart rhythm successfully reestablished in all cases), NS-VT = Non-sustained ventricular tachycardias, SD = Sudden Death.

| Animal No. | Maximum. HF power (Watts) | Duration (seconds) | His amplitude (mV) | escape rate (beats/min) | Side effects | Outcome | Lesion diameter x depth (mm) |
|---|---|---|---|---|---|---|---|
| 1 | 100 | 140 | 0.15 | 72 | VF | sacrificed | 3x3 (acute) |
| 2 | 100 | 167 | 0.20 | 73 | none | sacrificed | 9x10 (acute) |
| 3 | 100 | 30 | 0.11 | 90 | NS VT | sacrificed | 8x1 (acute) |
| 4 | 100 | 10 | 0.12 | 90 | NS VT | SD day 11 | 10x2 (chronic) |
| 5 | 100 | 25 | 0.18 | 52 | NS VT | SD day 7 | 15x2 (chronic) |
| 6 | 60 | 25 | 0.25 | 92 | NS VT | SD day 6 | 20x3 (chronic) |
| 7 | 100 | 110 | 0.19 | 68 | VF | SD day 7 | No lesion found |

Unipolar His bundle electrogram amplitudes from the coaxial catheter prior to HF ablation ranged from 0.11 to 0.25 mV. Complete AV block was achieved in all 7 sheep, using a maximum power ranging from 60 to 100 Watts. A third-degree AV block was obtained in 5 of the sheep with a second degree AV block in 2 of the animals, and complete AV block resulting from the following HF application. No resumption of conduction was observed either during or at the end of the ablation session. The rate of escape rhythm ranged from 52 and 92 beats/min. On the sixth day, the standard ECG showed the presence of the third degree AV block in 4 of the surviving animals. These sheep died on the sixth, seventh and eleventh day. The pathology examinations revealed hemorrhage and necrosis, and fibrosis 3 weeks later in the surviving sheep.

### 3.2. Ventricular Sites (Table II)

Acute lesions, Photo 1, with diameters between 3 and 45 mm (mean $\pm$ SD = 10.3 $\pm$ 10) and depths between 1 and 15 mm (6.7 $\pm$ 3.9), show a good correlation between the level of HF energy delivered and the dimensions of the lesions.

Visual inspection reveals hemorrhage and coagulation necrosis. No coagulum was seen at the ablation site. Chronic lesions were small in depth (1-4 mm) and diameter (7-20 mm). The characteristics, parameters and results of the HF application are summarized in Table 1. Intracardiac ablation was attempted in 10 sheep.
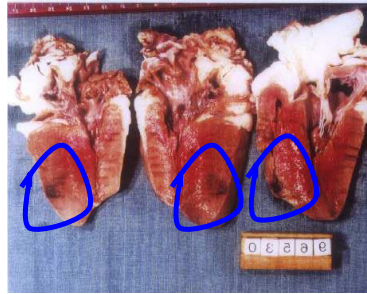
Photo 1. Lesions in the ventricle.

Table 2. Biophysical parameters and results for the different sheep in regard to all ablation sites except for atrioventricular junction, VF = Ventricular Fibrillation, VPB's = ventricular premature beats, AVB = Complete AV Block, NS-VT = Non-Sustained Ventricular Tachycardia.

| Animal No. | Max. power (watt) | Duration (seconds) | Side effects | Creatine before HF micromole/liter | Kinase 4h after HF micromole/liter | Outcome | Maximum lesion diameter x depth (mm) |
|---|---|---|---|---|---|---|---|
| 1 | 90 | 25 | VF | 133 | 478 | Sacrificed | 45x13 (acute) |
| 2 | 90 | 5 | VF | 170 | 250 | Sacrificed | 9x15 (acute) |
| 3 | 90 | 21 | VF | 162 | 1041 | Sacrificed | 15x7 (acute) |
| 4 | 50 | 40 | VPB's | 178 | 224 | SD day 11 (AVB) | 8x2 (chronic) |
| 5 | 20 | 30 | - | 89 | 88 | SD day 7 (AVB) | 5x1 (chronic) |
| 6 | 20 | 25 | VF | 115 | 254 | SD day 6 (AVB) | 20x2 (chronic) |
| 7 | 20 | 20 | NS-VT | 112 | 90 | SD day 7 (AVB) | 15x1 (chronic) |
| 8 | 30 | 75 | NS VT | 125 | 110 | Sacrificed at day 21 | 12x5 (acute) |
| 9 | 30 | 50 | VF | 90 | 105 | sacrificed at day 21 | 10x3 (chronic) |
| 10 | 30 | 60 | VF | 108 | 100 | sacrificed at day 21 | 7x4 (chronic) |

### 3.3. Side effects

During HF ablation at the ventricular sites, ventricular arrhythmias including ventricular premature beats, monomorphic and polymorphic non-sustained ventricular tachycardia (VT) were observed. In 6 cases VT led to ventricular fibrillation, requiring DC cardioversion. These arrhythmias were transient, lasting up to 3 minutes. Sudden death occurred in four animals and may be related to ventricular proarrhythmic effects. However, sudden death was observed in the sheep that had undergone AV ablation, which is likely to be responsible for lethal arrhythmias. Pathological examination of 2 animals that encountered sudden death at day 6 and 7, shows a slight pericardial inflammation. The two animals died probably because of the complete AV block. We had not considered it necessary to implant a pacemaker since the heart rate was considered to be satisfactory. However, adherence to the right ventricular wall was observed after application of 18 watts. Withdrawal and visual examination of the catheter did not reveal any thrombus.

### 4. Discussion

Only one renal complication, most likely linked to an embolism, was observed in this study. This is a well-known complication of RF energy, requiring a special preventive anticoagulant when ablation involves cauterization effects. This preventive therapy was not used in this study. Results indicate that HF energy induced non-sustained ventricular

arrhythmias, which led to ventricular fibrillation in 6 cases. For the moment, we have no solution to this problem.

The high number of ventricular fibrillations constitutes a temporary setback for the use of this technique in clinical applications; however, the procedure shows good HF wave diffusion. On the other hand, it is possible that the animal model was particularly susceptible to ventricular arrhythmias. The method for this study is currently undergoing validation.

Power levels used show a close correlation between the output and the dimensions of the lesions obtained. Table II shows that a 20 Watts power application easily results an atrioventricular block. The frequency (27.12 MHz) belongs to the ISM (Industry, Science, Medical) spectrum and its use is subject to official approval. Also available are 13.56 MHz, 434 MHz, 915 MHz and 2450 MHz. The 27.12 MHz wavelength $\lambda\acute{n} = 11.06$m which, when divided by the square root of $\varepsilon'_t$ (113 for the cardiac muscle) gives $\lambda_t = 1.1$ m, the wavelength in tissue. The electrode is 7 mm long and 2.5 mm in diameter which explains why the major part of energy is dissipated in a near field. This frequency induces two types of tissue heating. The first is conductive and produced by RF; the second is induced by the signal radiated by the electrode. The frequency-induced radiation, compared with the RF method, is to the advantage of our method as the HF method is less dependent on the quality of the electrode-tissue contact, which is determining for RF energy ablation [27]. The field radiated by the HF electrode is a near field [28]; the maximum radiated power is confined to less than one centimeter around the electrode, thus presenting no risk of dispersion.

## 5. Conclusion

This experimental sheep study suggests that large lesions can be obtained by means of HF energy using a 7F coaxial catheter connected to a specially designed generator. This type of energy produces a necrosis of the endocardium, enabling deep heating of the ventricular muscle. The frequency used renders the ablation less dependent on the electrode-tissue contact. Chronic lesions appear well demarcated from the adjacent myocardium, without perforations despite the high power output utilized.

## References

[1] Huang, S.K., Bharati, S., Graham, A.R. (1987). Closed chest catheter desiccation of the atrioventricular junction using radio frequency energy: a new method of catheter ablation. *J. Am. Coll. Cardiol*., 18, 349-358.

[2] Lavergne, T., Guize, L., Le Heuzey, J.Y. (1986). Closed-chest atrioventricular junction ablation by high-frequency energy transcatheter desiccation. *Lancet*, 2, 858-859.

[3] Wtorek, J., Bujnowski, A., Rumiński, J., Poliński, A., Kaczmarek, M., Nowakowski, A. (2012). Assessment of cardiovascular risk in assisted living. *Metrol. Meas. Syst.,* 19(2), 231-244.

[4] Jackman, W.M., Wang, X.Z., Friday, K.J. (1991). Catheter ablation of accessory atrioventricular pathways (Wolf-Parkinson-White syndrome) by radio frequency current. *N. Engl. J. Med.,* 324, 1605-1611.

[5] Jackman, W.M., Beckman, K.J., McClelland, J.H. (1992). Treatment of supraventricular tachycardia due to atrioventricular nodal re-entry by radio frequency catheter ablation of slow-pathway conduction. *N. Engl. J. Med.,* 327, 313-318.

[6] Haines, D.E., Verow, A. (1990). Observations on electrode-tissue interface temperature and effect on electrical impedance during radiofrequency ablation of ventricular myocardium. *Circulation,* 82, 1034-1038.

[7] Cooper, J.M., et al. (2004). Ablation with an internally irrigated radiofrequency catheter: learning how to avoid stem pops. *Heart Rhythm*, 1(3), 323-333.

[8]     Saxon, L.A., Natterson, P., Delurgio, D.D., Shannon, K. (1995). Impedance characteristics of retrograde versus transeptal approaches to radiofrequency ablation of the left sided accessory pathway (abstract). *PACE*, 18, 921.

[9]     Haines, D.E., Verow, A. (1990). Observations on electrode-tissue interface temperature and effect on electrical impedance during radiofrequency ablation of ventricular myocardium. *Circulation*, 82, 1034-1038.

[10]    Wittkampf, F., Simmers, T., Hauer, R., De Medina, E.R. (1995). Myocardial temperature response during radiofrequency catheter ablation. *PACE*, 18, 307-317.

[11]    Martinek, M. (2010). Identification of a high-risk population for esophageal injury during radiofrequency catheter ablation of atrial fibrillation: procedural and anatomical considerations. *Heart Rhythm*, 7(9), 1224-1230.

[12]    Ren, J.F., et al. (2004). Left atrial thrombus associated with ablation for atrial fibrillation: identification with intracardiography. *J. of the American college of cardiology*, 43(10), 1861-1867.

[13]    Zhou, L., et al. (1999). Thromboembolic complications of cardiac radiofrequency catheter ablation. A review of the reported incidence pathogenesis and current research directions. *J. Cardiovasc, Electrophysiol*, 10, 611-620.

[14]    Kok, L.C., et al. (2002). Cerebrovascular complications associated with pulmonary vein ablation. *J. Cardiovasc, Electrophysiol*, 13, 764-767.

[15]    Contreras-Valdes, F.M. (2011). Severity of esophageal injury predicts time to healing after radiofrequency catheter ablation for atrial fibrillation. *Heart Rhythm*, 8(12), 1862-1868.

[16]    Nakagawa, H., Yamanashi, W.S., Pitha, J.V. (1995). Comparison of in vivo temperature profile and lesion geometry for radiofrequency ablation with a saline-irrigated electrode versus temperature control in a canine thigh muscle preparation. *Circulation,* 91, 2264-2273.

[17]    Jaïs, P., Haïssaguerre, M., Shah, D.C., et al. (1998). Successful irrigated-tip catheter ablation of atrial flutter resistant to conventional radiofrequency ablation. *Circulation,* 98, 835-838.

[18]    Dubuc, M., Skanes, A., Roy, D., Thibault, B., Talajic, M., Guerra, P. (2000). Catheter cryomapping and cryoablation of supraventricular rachycardia in man: preliminary results (abstract). *PACE,* 23(II), 613.

[19]    Lesh, M.D., Diedrich, J., Guerra, P.G., Goseki, Y., Sparks, P.B. (1999). An anatomic approach to prevention of atrial fibrillation: Pulmonay vein isolation with through-the-ballon Ultrasound ablation. *Thorac. Cardiovasc. Surg.*, 47 (Suppl.), 347-351.

[20]    Svenson, R., Littman, L., Splinlen, R. (1990). Application of lasers for arrhytmia ablation. In Zipes D.; Jalife J. (eds): *Cardiac Electrophysiology from cell to Beside*. Philadelphia, WB Saunders, 989-997.

[21]    Splitzer, S.G., Richter, P., Knaut, M., Schuler, S. (1999). Treatment of atrial fibrillation in open heart surgery. The potentiel role of microwave energy. *Thorac. Cardiovasc. Surg.*, 47 (Suppl.), 374-378.

[22]    Adragao, P., Parreira, L., Morgado, F., Bonhorst, D., Seabra-Gomes, R. (1999). Microwave ablation of atrial flutter. *PACE*, 22, 1692-1695.

[23]    Vanderbrink, B.A., Gilbride, C. (2000). Safety and efficacy of a steerable temperature monitoring microwave catheter system for ventricular myocardial ablation. *J. Cardio. Electrophysiology*, 11, 305-310.

[24]    Rouane, A., Nadi., M., Bru, P., Staiquly, A., Kourtiche, D., Hedjiedj, A., Prieur, G. (1995). Intracardiac HF catheter ablatherapy: Technical aspects. *Med. Eng. Phys.,* 17, 36-41.

[25]    Sied, M., Rouane, A., Chapelon, P.A., Nadi, M., Bru, P. (1997). Study of Electrophysiological Monopolar and Bipolar Probes in Intracardiac HF Ablation Therapy. *ITBM*, 18, 219-223. (in French)

[26]    Rouane, A., Kourtiche, D. (2012). Characterization of microwave antennas for intracardiac ablation frequencies 915 and 2450 MHz. *Measurement Science Review*, 12(1), 34-39.

[27]    Haines, D.E. (1991). Determinants of lesion size during radiofrequency catheter ablation: the role of electrode-tissue contact pressure and duration of energy delivery. *J. Cardiovasc. Electrophysiol*, 2, 509-515.

[28]    Casey, J.P., Bansal, R. (1986). The near field of an insulated dipole in a dissipative dielectric medium. *IEEE Trans. Microwave Theory Tech.*, 34, 459-463.